

## Geodynamic interpretation of the heat flow in the Tyrrhenian Sea *Interpretazione geodinamica del flusso di calore nel Mar Tirreno*

MONGELLI F. (\*), ZITO G. (\*), DE LORENZO S. (\*), DOGLIONI C. (\*\*)

**ABSTRACT** - The higher heat flow in the eastern Tyrrhenian Sea supports both the notion of a migrating rift and an eastward migrating asthenosphere underneath the basin. Punctuation of the Tyrrhenian backarc extension in lithospheric boudins is accompanied by increase in heat flow generated by asthenospheric intrusions progressively moving eastward. The rifting developed in a pre-existing thickened lithosphere by the Alpine orogeny. The present heat flow should then be imaged as a transient wave of values migrating eastward in time.

**KEY WORDS:** heat flow, asthenospheric intrusions, eastwards migration, Tyrrhenian Sea

**RIASSUNTO** - La mappa del flusso di calore nel Mar Tirreno mostra un valore regionale molto alto di 120 mW m<sup>-2</sup> e due forti massimi locali di 143 e 245 mW m<sup>-2</sup> in aree di recente attività tettonica e vulcanica.

Il rifting che ha generato il bacino di retro-arco tirrenico iniziò nell'Oligocene superiore (19-15 Ma) generando il bacino Ligure-Provenzale. Il rifting saltò ad est del blocco Sardo-Corso, procedendo a salti e generando nel Tirreno meridionale due bacini principali: Vavilov (7-3.5 Ma) e Marsili (1.7-1.2 Ma) caratterizzati dai due omonimi vulcani. L'alto valore regionale del flusso di calore viene interpretato come conseguenza dell'assottigliamento litosferico mentre i due massimi locali vengono spiegati come intrusioni astenosferiche. Questa interpretazione supporta l'idea di un rift e di una astenosfera migranti entrambi verso est, accompagnate da intrusioni astenosferiche che si succedono l'una all'altra nella stessa direzione.

**PAROLE CHIAVE:** flusso di calore, intrusioni astenosferiche, migrazione verso est, Mar Tirreno

### 1. - INTRODUCTION

The Tyrrhenian Sea is an area of great interest from a geothermal point of view because the observed heat flow is one of the highest in the world.

ERICKSON (1970) carried out the first measurements of heat flow in the Tyrrhenian basin in 12 stations. The average value of the best 10 sites was 147.5 mW m<sup>-2</sup>.

SCLATER (1972) studied the relationship between heat flow and elevation of the marginal basins of the western Pacific, and LODDO & MONGELLI (1974) pointed out that Erickson's value was too high with respect to the elevation, denoting an anomalous state of the basin.

MALINVERNO (1981) & MALINVERNO *et alii* (1981) interpreted the existing data by supposing that the Tyrrhenian basin was created behind an eastward migrating trench system by the stretching of the lithosphere.

HUTCHISON *et alii* (1985) produced new heat flow data and applied the simple stretching model of MCKENZIE (1978) to the western Tyrrhenian (HF=1348±8 mW m<sup>-2</sup>) and obtained a very high stretching factor ( $\beta=6$ ). They maintain that, when stretching is long and continuous, oceanic crust is created in the central rift. They modeled this phase in the southern Tyrrhenian where the heat flow was 151±10 mW m<sup>-2</sup>, with the oceanic plate model of PARSONS & SCLATER (1977) which corresponds to  $\beta=\infty$ .

(\*) Dipartimento di Geologia e Geofisica, Università di Bari, Italy

(\*\*) Dipartimento di Scienze della Terra, Università "La Sapienza", Roma, Italy

DELLA VEDOVA *et alii* (1991) compiled a heat flow map of the Tyrrhenian Sea and surrounding areas based both on pre-existing data and new measurements. This map (fig. 1) shows a very high regional value of  $120 \text{ mW m}^{-2}$  and two strong local maxima of  $143 \text{ mW m}^{-2}$  and  $245 \text{ mW m}^{-2}$  in areas of recent tectonic and volcanic activity and of probable convective water movements.

Since new geological and geophysical knowledge has accumulated on the basin, we propose an updated geodynamic interpretation of the heat flow.

## 2. - GEOLOGICAL AND GEOPHYSICAL SETTING

Research about the geological history of the Tyrrhenian Sea has greatly improved due to some DSDP and ODP wells, seismic reflection profiles, sampling and volcanological studies (e.g., ZITELLINI *et alii*, 1986; ELLAM *et alii*, 1988; KASTENS *et alii*, 1988; FRANCALANCI *et alii*, 1993; PASCUCCI *et alii*, 1999). Several papers proposed geophysical and geodynamic models on the opening of the basin (e.g., SCANDONE, 1980; MALINVERNO *et alii*, 1981; MANTOVANI, 1982;

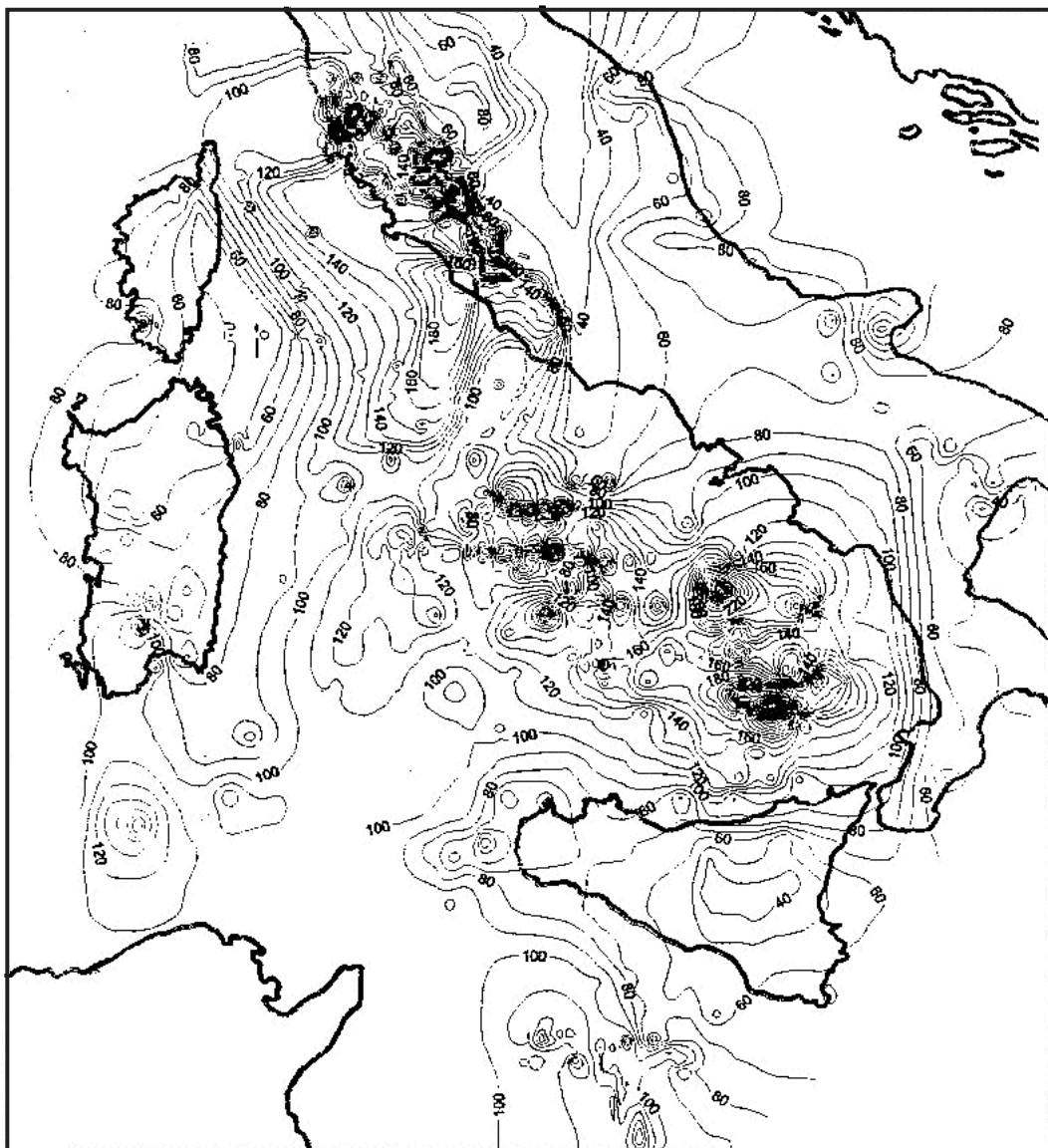


Fig. 1 – Heat flow density ( $\text{mW m}^{-2}$ ) in the Italian Peninsula and surrounding areas (Contour lines equidistance:  $10 \text{ mW m}^{-2}$ )

FINETTI & DEL BEN, 1986; MALINVERNO & RYAN, 1986; PATACCA & SCANDONE, 1989; MONGELLI & ZITO, 1994; GUEGUEN *et alii* 1997; CELLA *et alii*, 1998). Here we summarize some important results that are useful for our study.

The Adriatic microplate subduction initiated in the Late Oligocene-Early Miocene and developed to the East of the former Alpine Chain. The Apenninic accretionary prism formed in sequence at the front of the pre-existing Alpine back-thrust belt. The Apenninic back-arc extension migrated eastward and boudinated the former Alpine nappe stack (DOGLIONI *et alii*, 1998). Kinematics and geophysical data support the presence of an eastward migrating asthenospheric wedge at the subduction hinge of the rolling-back Adriatic plate (GUEGUEN *et alii*, 1997).

Rifting initiated in the Upper Oligocene in the Liguro-Provençal basin to the west of Corsica-Sardinia, floored by oceanic crust 19-15 Ma ago. The rifting jumped east of Corsica and Sardinia proceeding by steps and generating in the southern Tyrrhenian two major basins, i.e., the Vavilov basin (7-3.5 Ma) and the Marsili basin (1.7-1.2 Ma) marked by the two homonymous volcanoes Vavilov and Marsili (fig. 2).

Basalts at the Mt Vavilov are OIB-MORB type with an age of 4.1 Ma (SARTORI, 1989), while the basalts of Mt. Marsili are calc-alkaline (BECCALUVA *et*

*alii*, 1990), and the upper-lying sediments have an age of 1.8 Ma (KASTENS *et alii*, 1988) indicating a very young basaltic crust.

Subduction of the southern Adriatic plate is demonstrated by the existence of a well-defined Benioff plane under the Tyrrhenian Sea. Many authors (GASPARINI *et alii*, 1982; ANDERSON & JACKSON, 1987; GIARDINI & VELONÀ, 1991; AMATO *et alii*, 1991, 1993; SELVAGGI & CHIARABBA, 1995; CIMINI, 1999; SELVAGGI, 2001) have attempted to define the geometry of the subducted slab by different seismological methods. SELVAGGI & CHIARABBA (1995) described a continuous slab having a gentle slope down to 50 km of depth, then a rapid increase at the hinge, where the slope reaches 70° that remains constant down to 500 km.

CALCAGNILE & PANZA (1981) defined the lithosphere thickness of the Tyrrhenian area by the dispersion of surface waves; they found that the lithosphere is thinned up to 30 km in the central sector of the area. Recently PONTEVIVO & PANZA (2002) found that the thickness is about 20 km in the southernmost sector of the basin (fig. 3). The structure of the Tyrrhenian crust has been studied at length by gravimetric methods (MORELLI, 1970, 1981; MORELLI *et alii*, 1975) and seismic exploration (FINETTI & DEL BEN, 1986; PASCUCCI *et alii*, 1999).

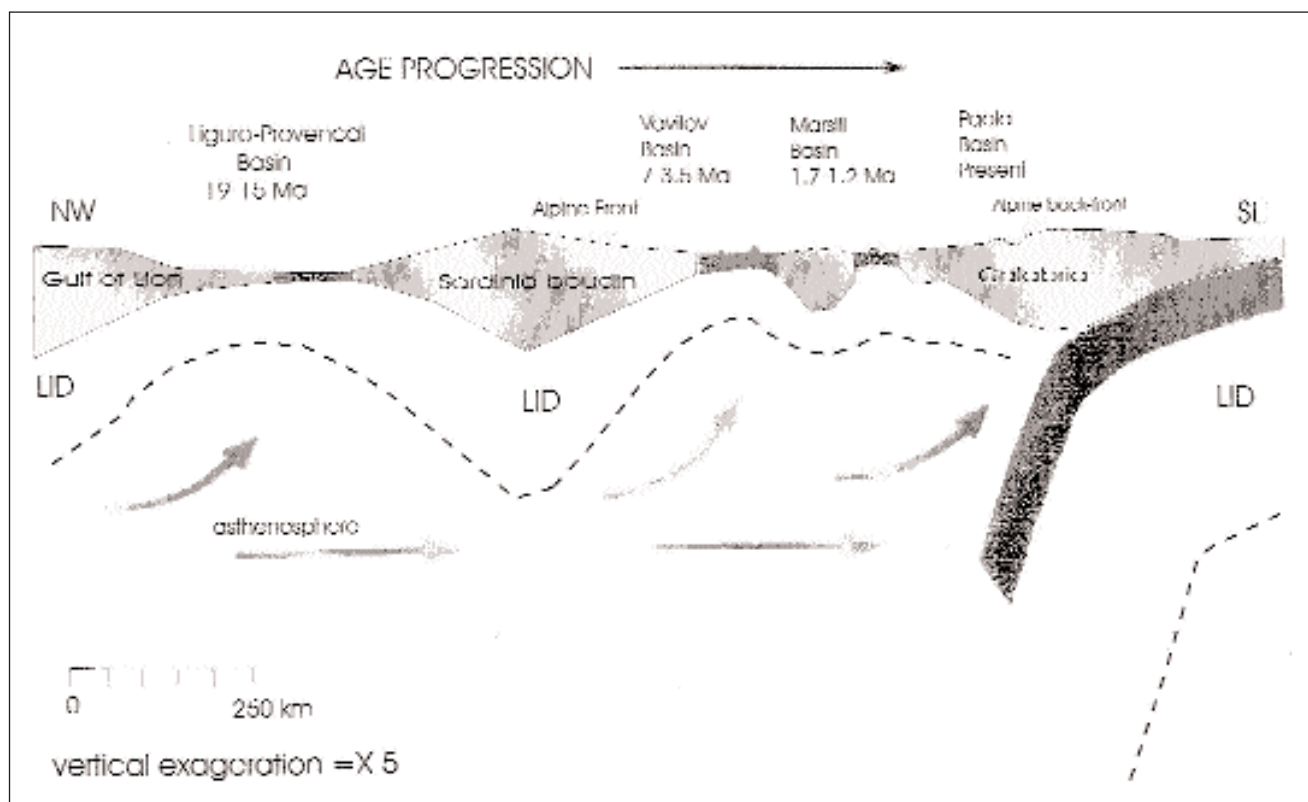


Fig. 2 – The progressive boudinage and deformation of the Alpine belt by the back-arc extension of the Apenninic subduction (by GUEGUEN *et alii*, 1999)

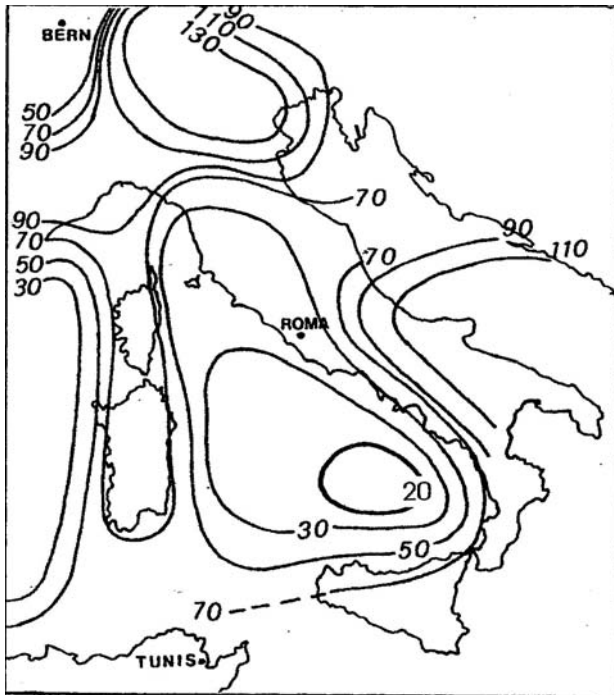


Fig. 3 – Lithospheric thickness (km) in Italian territory and surrounding areas (CALCAGNILE & PANZA, 1980, modified after the results of PONTEVIVO & PANZA, 2002)

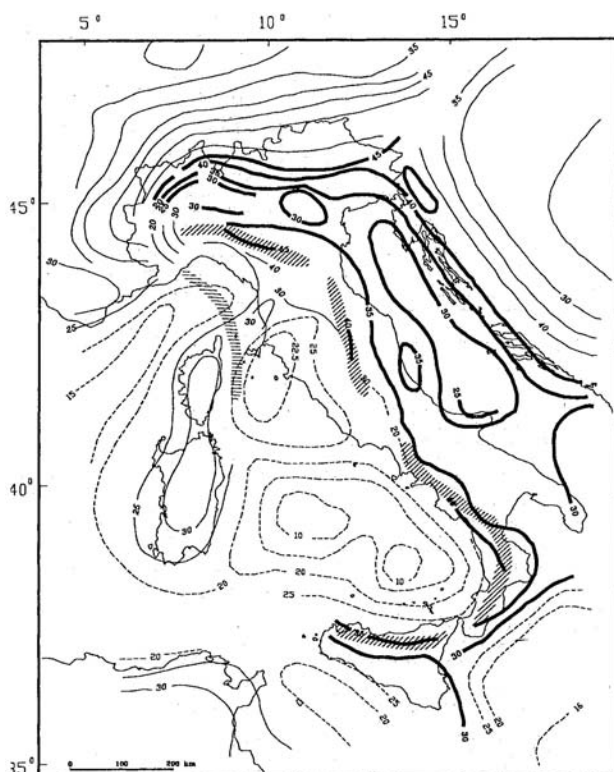


Fig. 4 – Moho isobaths (km) in Italian territory and surrounding areas. Different contour lines are ascribed to the Adriatic plate -thick lines-; the European plate -thin lines- and the stretched continental crust -dashed lines- (after LOCARDI & NICOLICH, 1988, modified).

The Tyrrhenian Sea is the site of an intense Bouguer anomaly ( $>250$  mGal); its interpretation (CELLA *et alii*, 1998) by assuming density values constrained by the results of the seismic exploration, confirms the existence of a very thin crust (fig.4).

The map of the depth of the Moho (LOCARDI & NICOLICH, 1988 modified by MORELLI, 1995) shows values lower than 15-20 km for the bathial plane, and two minima of 10 km centered on the Vavilov and Marsili basins. It is worthwhile to note that these minima coincide with the highest values of the heat flow. The lithospheric boudinage proposed by GUEGUEN *et alii* (1997) and shown as figure 2 is suggested to be slightly asymmetric by the gravimetric reconstruction of CELLA *et alii* (1998), the continental roots of Corsica-Sardinia being shifted to the east with respect to the higher topography. This would confirm the presence of a migrating asthenosphere from west to east.

### 3. - THE MODEL OF THE TYRRHENIAN SEA FORMATION

#### 3.1. - GEODYNAMIC MODEL

Let suppose that during Oligocene time, the European and Adriatic plates are sutured by the Alpine orogen giving a thickened lithosphere  $h_L$ , ideally composed of two sectors BC and CD, to the East of a sector AB of the Alpine foreland with thickness  $L$  (fig. 5).

In early Miocene time, between 19 and 15 Ma ago, sector AB first stretched by a factor  $\beta$  so that it thinned to  $L/\beta$ . Further stretching caused the laceration of the thinned lithosphere favouring the passive rising at the surface of an asthenospheric body wide  $a$ . As a consequence, blocks BC+CD rifted by AB  $(\beta-1)+a$ .

During Late Miocene-Early Pliocene times between 7 and 3.5 Ma ago, sector BC stretched by the factor  $\beta_1$ , and thinned to  $h_L/\beta_1$ . At 3.5 Ma ago, further stretching caused the laceration of the thinned lithosphere favoring the passive rising of an asthenospheric body, wide  $b$ . As a consequence, block CD further rifted by BC  $(\beta_1-1)+b$ .

During Pleistocene times, between 1.7 and 1.2 Ma ago, block CD stretched by the factor  $\beta_2$  and thinned to  $h_L/\beta_2$ . At 1.2 Ma ago further stretching caused the laceration and the rising of an other asthenospheric body, wide  $c$ . Point D further rifted by CD  $(\beta_2-1)+c$ . These last two extensions formed the southern Tyrrhenian Sea.

At present, the distance BD is about 550 km, that is the distance between Sardinia and Calabria.

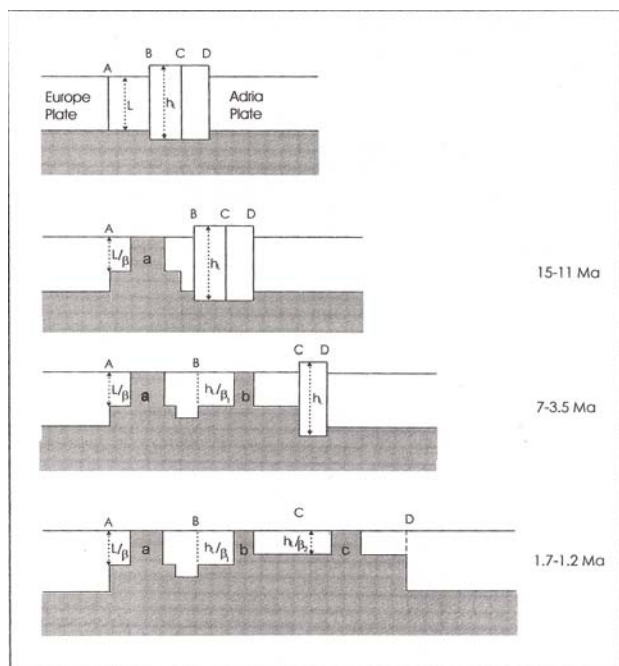


Fig. 5 – Diagrammatic illustration of the time evolution of the lithospheric extension and thinning, since Oligocene to Pleistocene. See text for explanation.

### 3.2. - THERMAL MODEL

Figure 6 shows the heat flow map of the Tyrrhenian Sea, which has been smoothed to eliminate small local anomalies. This map is the result of the superimposition of the effects of the lithospheric extension and of local asthenospheric intrusions in two different areas: the older Vavilov basin, where heat flow reaches the value of  $140 \text{ mW m}^{-2}$ , and the younger Marsili basin, with values of  $240 \text{ mW m}^{-2}$ .

From a thermal point of view, we have to consider the mantle, the radioactive components of the heat flow, and the intrusion effects.

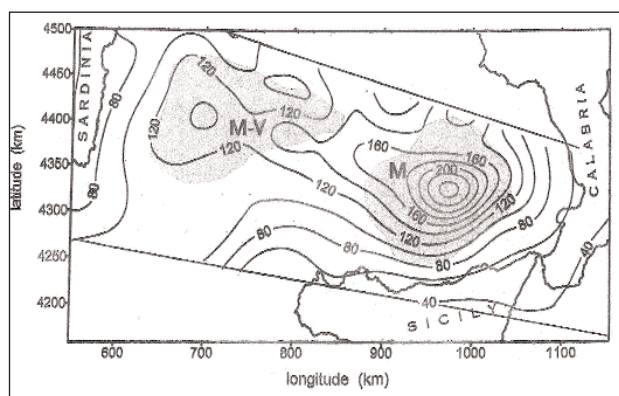


Fig. 6 – The smoothed heat flow density map (in  $\text{mW m}^{-2}$ ) of the Southern Tyrrhenian Sea.

#### 3.2.1 - Mantle component

MC KENZIE (1978) showed that the mantle component of the temperature and heat flow in a basin after a sudden passive pure shear extension, taking the surface temperature equal to zero, are respectively:

$$T(z, t) = T_1 \left\{ 1 - \frac{z}{h_L} + \frac{2}{\pi} \sum_{n=1}^{\infty} \frac{(-1)^{n+1}}{n} \left[ \frac{\beta}{n\pi} \sin\left(\frac{n\pi}{\beta}\right) \right] \sin\left(\frac{n\pi}{h_L} z\right) \exp\left(-\frac{n^2 t}{\tau}\right) \right\} \quad (1)$$

$$q_w = \lambda \frac{T_1}{h_L} \left[ 1 + 2 \sum_{n=1}^{\infty} \left[ \frac{\beta}{n\pi} \sin\left(\frac{n\pi}{\beta}\right) \right] \exp\left(-\frac{n^2 t}{\tau}\right) \right] \quad (2)$$

where the thermal conductivity of the lithosphere  $T_1$  the temperature at the base of the lithosphere  $h_L$  the thickness of the lithosphere before thinning  $\beta$  the thinning factor of the lithosphere

$$\tau = \frac{h_L^2}{\pi^2 \kappa}$$

$\kappa$  the thermal diffusivity of the lithosphere

$\tau$  the time after the thinning

$\lambda T_1 / h_L$  is the mantle heat flow before thinning.

We assume that before the extension phase the lithosphere had the same structure as the present Alpine Chain (because it was part of this chain): a lithosphere 130 km thick (CALCAGNILE & PANZA, 1980) and a crust 45-50 km thick (LOCARDI & NICOLICH, 1988; MORELLI, 1995).

To calculate values in both basins we use the numerical relation (MONGELLI, 1991) which expresses the rethickening after stretching

$$\frac{h_t - h}{h_L} = 0.0109 + \left(1 - \frac{1}{\beta}\right) 0.99 \exp\left(-\frac{10t}{\beta\tau}\right) \quad (3)$$

where  $h$  is the lithospheric thickness at the time  $t$  after extension.

We obtain  $\beta_1 = 6.3$  for the older extension and  $\beta_2 = 7.0$  for the younger.

We assume  $T_a = 1330^\circ\text{C}$ ,  $\kappa = 25.3 \text{ km}^2 \text{ Ma}^{-1}$ ,  $\lambda = 2.5 \text{ Wm}^{-1} \text{ K}^{-1}$  (ZITO *et alii*, 1993). The mantle contribution to the heat flow before thinning is  $25.6 \text{ mW m}^{-2}$ .

Figure 7 shows the mantle component of the geotherms to both extensions at present. Figure 8 shows the evolution of the heat flow; it is possible to see that at present, the value relative to the first extension is  $135 \text{ mW m}^{-2}$ , while that relative to the second extension is  $205 \text{ mW m}^{-2}$ .

#### 3.2.2 - Radioactive component

The radioactive component of the heat flow in the Tyrrhenian basin can be deduced from the crust structure of the Alps. As the result of continent-

continent underthrusting, the crust under the Alps is a doubled crust (PFINNER, 1990; YE & ANSORGE, 1990).

CERMAK & BODRI (1991, 1996) modeled the thermal evolution of the Alps by assuming an exponential distribution of heat production in each crust component. As the total crust is 50 km thick, we assume each crust component 25 km thick. This crust under the central Tyrrhenian sea is reduced, by extension, to 15 km thick by a factor  $\beta_c=3.3$ , and each crust component to  $H_r=7.5$  km.

In the southernmost sector the crust is reduced to 10 km by a factor of  $\beta_c=5$  and each crust component to  $H_r=5$  km. As a consequence, the contribution of radioactivity to the surface heat flow is strongly reduced. We retain that, in a short time the contribution is near the equilibrium. For simplicity, we calculate the thermal contribution of the radioactivity of this thinned crust in steady state.

We solve the equation:

$$\frac{d^2 T_r}{dz^2} = -\frac{A(z)}{\lambda} \quad (4)$$

where:

$$A(z) = \frac{A_0}{\beta_c} \exp\left(-\frac{z}{D}\right) \quad 0 < z < H_r$$

$$A(z) = \frac{A_0}{\beta_c} \exp\left(-\frac{z-H_r}{D}\right) \quad H_r < z < \frac{h_1}{\beta}$$

that is we assume that the pre-extension radioactive heat production  $A_0=3.15 \mu\text{Wm}^{-3}$  is depleted by the factor  $\beta_c$ . Moreover  $D=8$  km,  $h_1/\beta_1=30$  km,  $H_r=7.5$  km for the older basin, and  $h_1/\beta_2=20$  km and  $H_r=5$  km for the younger.

With the boundary conditions:

$$T_r(z=0) = T_r\left(z = \frac{h_1}{\beta}\right) = 0^\circ\text{C}$$

$$T_r(z=H_r) = T_r(z=H_r')$$

$$\left.\frac{dT_r}{dz}\right|_{z=H_r} = \left.\frac{dT_r}{dz}\right|_{z=H_r'}$$

we have the solution given in Appendix (A1).

Figure 9 shows the radioactive component of the geotherms relative to both extensions. From the solution (A3) in the Appendix, we have the surface heat flow given by:

$$\lambda \left.\frac{dT_r}{dz}\right|_{z=0} = \frac{A_0 D z_1}{\beta_1 z_2} \left[ \exp\left(-\frac{z_1}{D}\right) - 1 \right] + \frac{A_0 D^2}{\beta_1 z_2} \left[ \exp\left(-\frac{(z_2 - z_1)}{D}\right) + \exp\left(-\frac{z_1}{D}\right) - 2 \right] + \frac{A_0 D}{\beta_1} \left[ 2 - \exp\left(-\frac{z_1}{D}\right) \right] \quad (5)$$

Thus, the contribution to the surface heat flow is  $7.95 \text{ mWm}^{-2}$ , for the older and  $6.2 \text{ mWm}^{-2}$  for the younger basin.

As a consequence the calculated surface heat flow of the first extension is about  $143 \text{ mWm}^{-2}$ , and that of the second extension is about  $213 \text{ mWm}^{-2}$ . It is worthwhile to remember that the present value of the heat flow in the area of the first extension is more than  $140 \text{ mWm}^{-2}$  whereas it is more than  $240 \text{ mWm}^{-2}$  in the eastward younger Marsili basin (fig.6). These values are attributable to the asthenospheric intrusions and seems to confirm that when  $\beta > 6$  laceration of the lithosphere occurs.

### 3.2.3 - Thermal effect of asthenospheric intrusion

We suppose that the asthenospheric intrusion reaches the surface and cools down. The magma has a melt temperature  $T_m$  at which the phase change from liquid to solid occurs. The position of the phase change boundary  $z_m$  moves downward as solidification proceeds and, moreover, at this interface latent heat of fusion  $L$  is liberated. This is the Stefan problem. The solution, in one dimension, is (TURCOTTE & SCHUBERT, 1982):

$$\frac{T(z,t) - T_0}{T_m - T_0} = \frac{\text{erf}\left(\frac{z}{2\sqrt{\lambda t}}\right)}{\text{erf}\lambda_1} \quad (6)$$

where  $T_0$  is the surface temperature,

$$\lambda_1 = \frac{z_m}{2\sqrt{\lambda t}} \quad (7)$$

and  $\lambda_1$  is determined by the transcendental equation:

$$\frac{\exp(-\lambda_1^2)}{\lambda_1 \text{erf}\lambda_1} = \frac{L\sqrt{\pi}}{c(T_m - T_0)} \quad (8)$$

where  $c$  is the specific heat.

The surface heat flow is:

$$\lambda \left.\frac{dT}{dz}\right|_{z=0} = \frac{\lambda}{\sqrt{\pi \lambda t}} \frac{T_m}{\text{erf}\lambda_1} \quad (9)$$

We retain that the second extension is so recent (1.2 Ma) that the one-dimension Stefan model may be applied to the central part of the basin.

We assume  $T_0=0^\circ\text{C}$ ,  $T_m=1330^\circ\text{C}$ ,  $c=1 \text{ kJkg}^{-1}\text{K}^{-1}$ ,  $L=400 \text{ kJkg}^{-1}$  and for ultrabasic rocks at  $1300^\circ\text{C}$  thermal conductivity  $\lambda=1.45 \text{ Wm}^{-1}\text{K}^{-1}$  (ZOTH & HAENEL, 1988) and the thermal diffusivity  $\kappa=21.5 \text{ km}^2 \text{ Ma}^{-1}$  (ZITO *et alii*, 1993).

From eq. (8) we obtain  $\lambda_1 = 0.932 \text{ Wm}^{-1}\text{K}^{-1}$  and  $\text{erf}(\lambda_1)=0.812$  figure 10 shows the geotherm in the second intrusion case. Figure 11 shows the variation of the surface heat flow in time, on which the value relative to the second intrusion is well fitted.

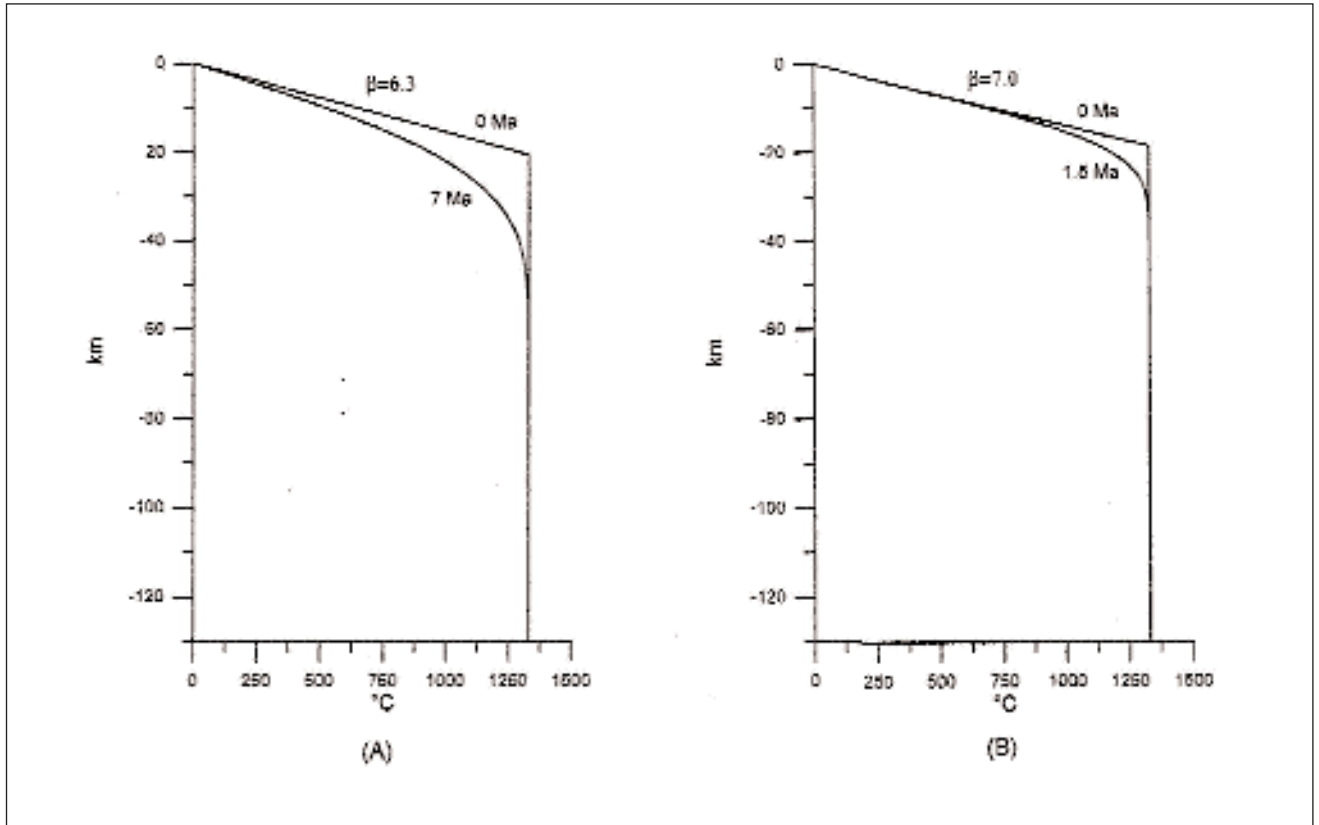


Fig. 7 – Present mantle component of the geotherms for the first (a) and second (b) extension.

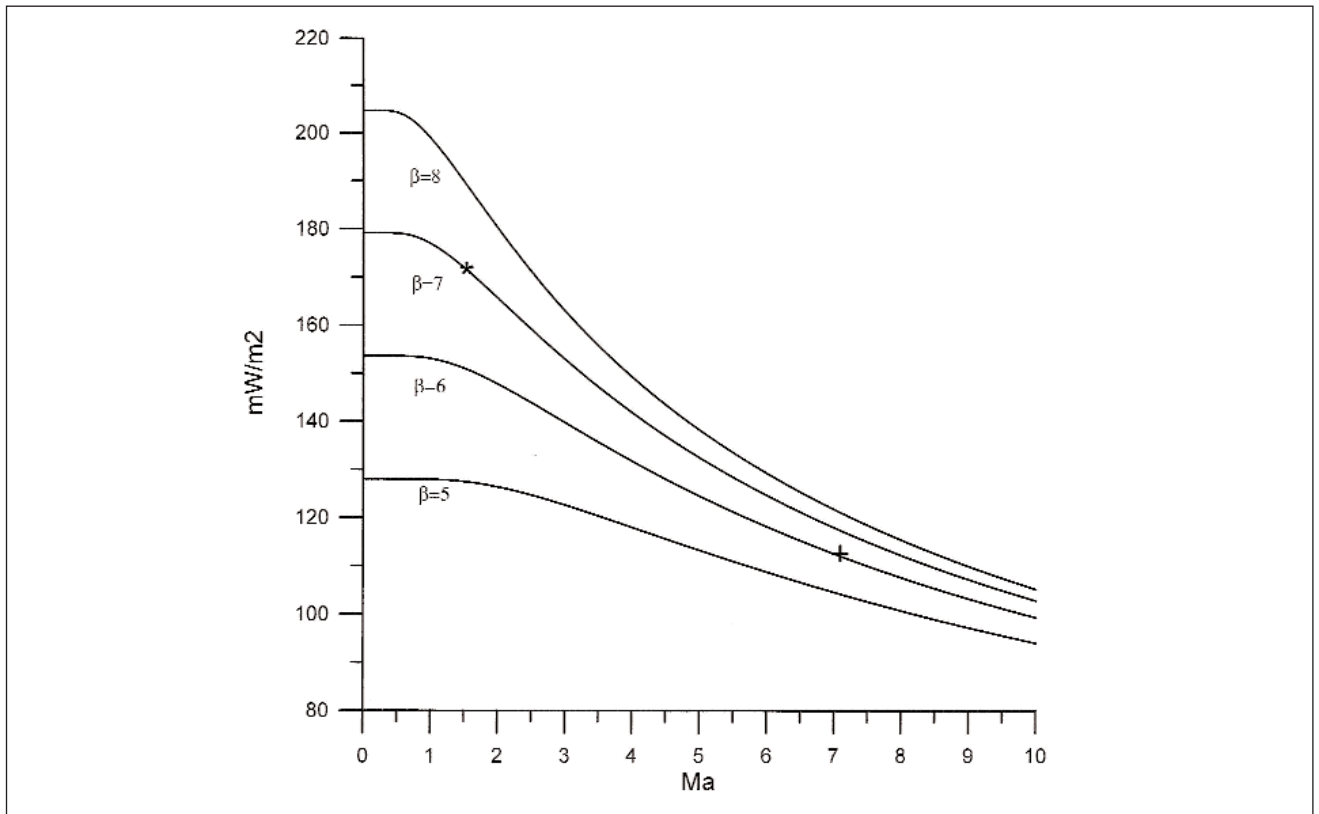


Fig. 8 – Time variation of the surface heat flow density ( $mW m^{-2}$ ) of a lithosphere stretched by different factor. Cross refers to the first extension; asterisk to the second extension.

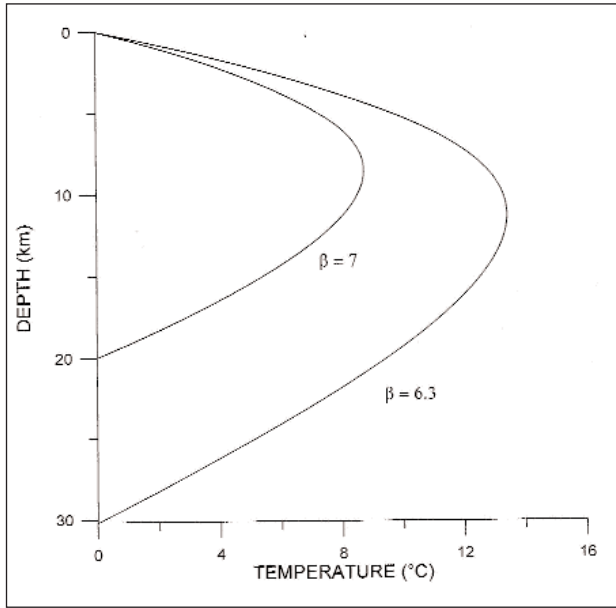


Fig. 9 – Radioactive component of the geotherms

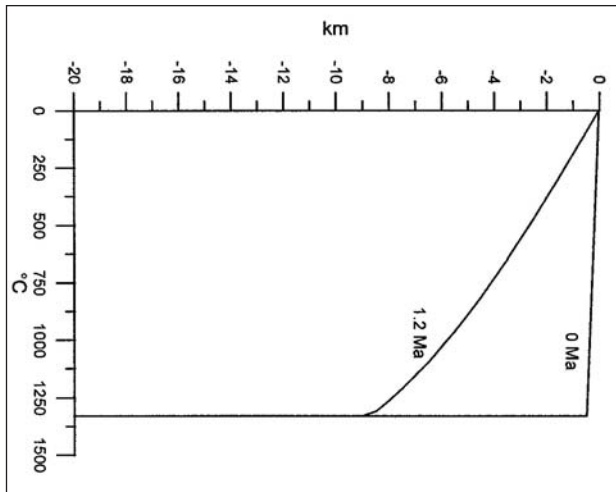


Fig. 10 – Present geotherm in the second intrusion beneath the Marsili basin.

From eq.(5), taking  $k=0.7 \text{ mm}^2/\text{s}$  we obtain  $z_m=7.0$  km. This is the thickness of the newly created lithosphere. Moreover, the contour 10 km below the Marsili basin in figure 4 indicates the thickness of the lithosphere.

The intrusion below the Vavilov basin is older, thus the new lithosphere is thicker. By assuming approximately the one-dimension solution, we obtain  $z_m=11.2$  km. Because the lateral loss of heat of the older intrusion,  $z_m$  is surely more than 11.2 km, we expect that within the new lithosphere, new thin oceanic crust is differentiated. In this case we retain that the contour of 10 km in figure 4 below the Vavilov basin indicates effectively the Moho depth.

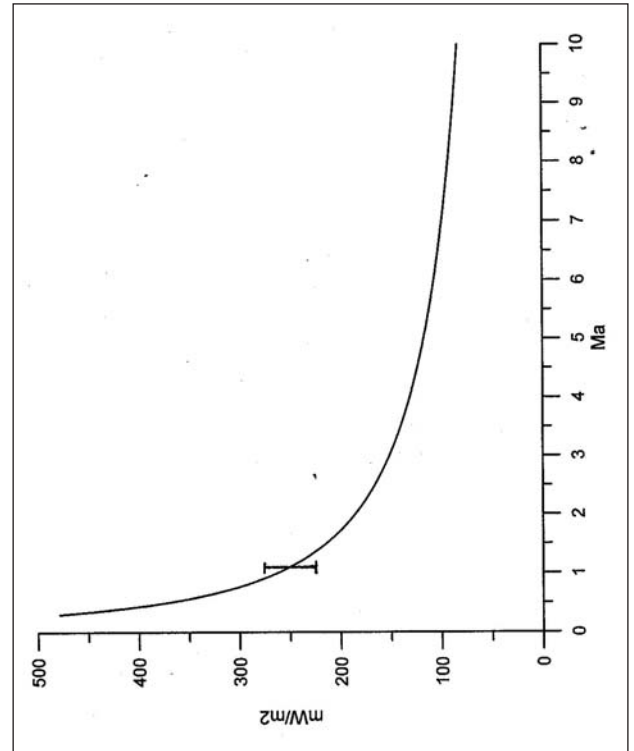


Fig. 11– Time variation of the surface heat flow ( $\text{mW m}^{-2}$ ) of an asthenospheric body according to the Stefan's equation (9). Error bar refers to the second intrusion under the Marsili basin

#### 4. - CONCLUSION

Figure 12 shows the thickness of the lithosphere along the sector of figure 6 and the geotherms in each sector calculated by using eqs. (1), A1 and (6). It is worthwhile to underline some interesting results deriving from this study:

- the opening of the southern Tyrrhenian basin occurred by two rapid and separate episodes which stretched the lithosphere by the factor  $\beta=6$ .
- further stretching generates the laceration of the lithosphere allowing the sudden passive rise of the asthenospheric materials which cools, liberates the latent heat of fusion and solidifies.
- new lithosphere is formed within the intrusion whose thickness is defined by the depth of the solidification boundary.
- the Moho depth in the Tyrrhenian basin has different origin: in the continental areas it is due to the stretching of the primitive crust-lithosphere, whereas within the intrusion it is a new oceanic one, formed by differentiation of the asthenospheric material.

It is generally accepted that extensional thinning of the lithosphere is due to stresses generated by boundary forces related to slab pull (e.g. FORSYTH & UYEDA, 1975; ANGELIER & LE PICHON, 1979) or to differential drag exerted by an eastward migrating

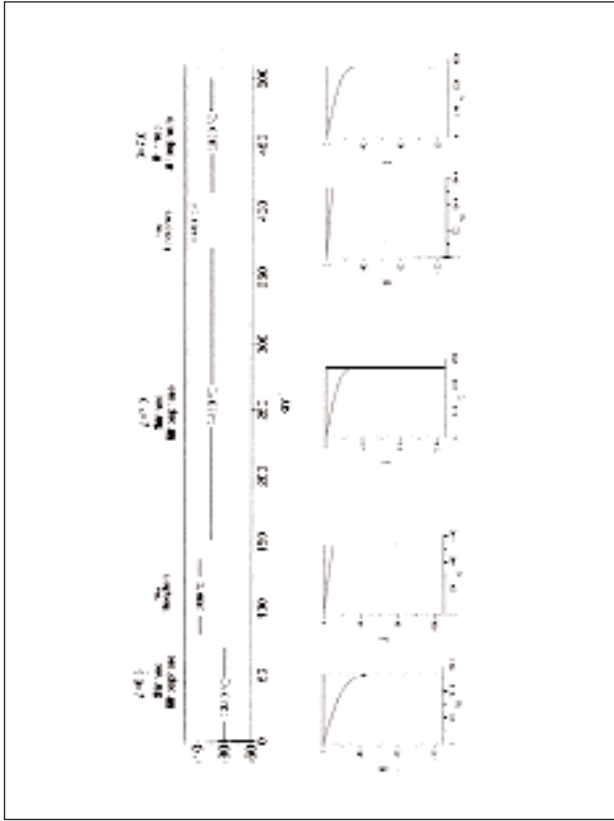


Fig. 12 – Present lithospheric thicknesses along the given profile and the respective geotherms.

mantle (DOGLIONI *et alii*, 1998). In these cases, extension may be related to the rate of subduction. Episodic backarc extension of the Tyrrhenian basin induces us to retain that the subduction rate is not continuous, or that stretching in the backarc is not continuous during a steady state subduction process. In fact, while the average rate deduced by the extension of the subducted slab (about 500 km) and its age (about 20 Ma) is about 2.5 cm/a, PATACCA *et alii*, (1990) estimated a rate of about 5 cm/a for the last Ma probably related to the second intrusion.

## APPENDIX

The solution of the steady state heat conduction equation:

$$\frac{d^2T}{dz^2} = -\frac{A(z)}{\lambda}$$

where:

$$A(z) = \frac{A_0}{\beta_1} \exp\left(-\frac{z}{D}\right) \quad 0 < z < z_1$$

$$A(z) = \frac{A_0}{\beta_1} \exp\left(-\frac{z-z_1}{D}\right) \quad z_1 < z < z_2$$

with the following boundary conditions:

$$T_r(z=0) = T_r(z=L) = 0^\circ\text{C}$$

$$T_r(z=H_1^-) = T_r(z=H_1^+)$$

$$\left.\frac{dT_r}{dz}\right|_{z=H_1^-} = \left.\frac{dT_r}{dz}\right|_{z=H_1^+}$$

is given by:

$$T(z) = \frac{A_0 D^2}{\beta_1 \lambda} \left[ 1 - \exp\left(-\frac{z}{D}\right) \right] + \frac{A_0 D z_1}{\beta_1 \lambda z_2} \left\{ \exp\left(-\frac{z_1}{D}\right) - 1 \right\} + \frac{z}{z_2} \frac{A_0 D^2}{\beta_1 \lambda} \left[ \exp\left(-\frac{(z_2-z_1)}{D}\right) + \exp\left(-\frac{z_1}{D}\right) - 2 \right] + \frac{A_0 D z_1}{\beta_1 \lambda} \left[ 1 - \exp\left(-\frac{z_1}{D}\right) \right] \quad 0 < z < z_1 \quad (A1)$$

$$T(z) = -\frac{A_0 D^2}{\beta_1 \lambda} \exp\left[-\frac{(z-z_1)}{D}\right] + \frac{A_0 D z_1}{\beta_1 \lambda z_2} \left[ \exp\left(-\frac{z_1}{D}\right) - 1 \right] + \frac{z}{z_2} \frac{A_0 D^2}{\beta_1 \lambda} \left[ \exp\left(-\frac{(z_2-z_1)}{D}\right) + \exp\left(-\frac{z_1}{D}\right) - 2 \right] + 2 \frac{A_0 D^2}{\beta_1 \lambda} \left[ 2 - \exp\left(-\frac{z_1}{D}\right) \right] + \frac{A_0 D z_1}{\beta_1 \lambda} \left[ 1 - \exp\left(-\frac{z_1}{D}\right) \right] \quad z_1 < z < z_2 \quad (A2)$$

$$\left.\frac{dT}{dz}\right|_{z=0} = -\frac{A_0 D}{\beta_1 \lambda} \exp\left(-\frac{z}{D}\right) + \frac{A_0 D z_1}{\beta_1 \lambda z_2} \left\{ \exp\left(-\frac{z_1}{D}\right) - 1 \right\} + \frac{A_0 D^2}{\beta_1 \lambda z_2} \left[ \exp\left(-\frac{(z_2-z_1)}{D}\right) + \exp\left(-\frac{z_1}{D}\right) - 2 \right] + \frac{A_0 D}{\beta_1 \lambda} \left[ 1 - \exp\left(-\frac{z_1}{D}\right) \right] \quad 0 < z < z_1$$

and the gradient is:

$$\left.\frac{dT}{dz}\right|_{z=0} = -\frac{A_0 D}{\beta_1 \lambda} \exp\left[-\frac{(z-z_1)}{D}\right] + \frac{A_0 D z_1}{\beta_1 \lambda z_2} \left\{ \exp\left(-\frac{z_1}{D}\right) - 1 \right\} + \frac{A_0 D^2}{\beta_1 \lambda z_2} \left[ \exp\left(-\frac{(z_2-z_1)}{D}\right) + \exp\left(-\frac{z_1}{D}\right) - 2 \right] + \frac{A_0 D}{\beta_1 \lambda} \left[ 1 - \exp\left(-\frac{z_1}{D}\right) \right] \quad z_1 < z < z_2$$

The surface gradient ( $z=0$ ) is:

$$\left.\frac{dT}{dz}\right|_{z=0} = -\frac{A_0 D}{\beta_1 \lambda} \exp\left(-\frac{z_1}{D}\right) + \frac{A_0 D z_1}{\beta_1 \lambda z_2} \left\{ \exp\left(-\frac{z_1}{D}\right) - 1 \right\} + \frac{A_0 D^2}{\beta_1 \lambda z_2} \left[ \exp\left(-\frac{(z_2-z_1)}{D}\right) + \exp\left(-\frac{z_1}{D}\right) - 2 \right] + \frac{A_0 D}{\beta_1 \lambda} \left[ 1 - \exp\left(-\frac{z_1}{D}\right) \right] \quad (A3)$$

## REFERENCES

- AMATO A., CIMINI C., ALESSANDRINI B. (1991) - *Struttura del sistema litosfera-astenosfera nell'Appennino Settentrionale da dati di tomografia sismica*. Studi Geologici Camerti, Vol. Spec. (1991/1), 83-90.
- ANDERSON H. & JACKSON J. (1987) - *The deep seismicity of the Tyrrhenian Sea*. Geophysical Journal of Royal Astronomical Society, v.91, pp. 613-637.
- ANGELIER J. & LE PICHON X. (1979) - *The Hellenic Arc and Trench system: a key to the tectonic evolution of the eastern Mediterranean*. Tectonophysics, **60**: 1-40.
- BECCALUVA L., BONATTI E., DUPUY C. *et alii* (1990) - *Geochemistry and mineralogy of volcanic rocks from the ODP*

- sites 650, 651, 655 and 654 in the Tyrrhenian sea. Proceedings of the ODP, *Scientific Results*, **107**: 49-74.
- CALCAGNILE G. & PANZA G.F. (1980) - Upper mantle structure of the Apulian plate from Rayleigh waves, *Pure appl. Geophys.*, **118**: 823-830.
- CALCAGNILE G. & PANZA G.F. (1981) - The main characteristics of the Lithosphere Asthenosphere System in Italy and surrounding regions. *Pageoph*, v.119, pp. 865-879.
- CELLA F., FEDI F., FLORIO G. & RAPOLLA A. (1998) - Optimal gravity modelling of the litho-asthenosphere system in Central Mediterranean. *Tectonophysics*. Vol. 287, Nos. 1-4, 117-138.
- CERMAK V. & BODRI L. (1991) - A heat production model of the crust and upper mantle. *Tectonophysics*, **194**: 307-323.
- CERMAK V. & BODRI L. (1996) - Time dependent deep temperature modelling: Central Alps. *Tectonophysics*, **257**: 7-24.
- CIMINI G.B. (1999) - P-wave deep velocity structure of the southern Tyrrhenian subduction zone from non-linear teleseismic travel time tomography. *Geoph. Res. Lett.*, **26** (24): 3709-3712.
- DELLA VEDOVA B., MONGELLI F., PELLIS G. & ZITO G. (1991) - Campo regionale del flusso di calore nel Tirreno. Ati 10° Convegno GNGTS, Esagrafo, Rora, 817-825.
- DOGLIONI C., MONGELLI F. & PIALLI G.P. (1998) - Boudinage of the Alpine belt in the Apenninic back-arc. *Mem. Soc. Geol. It.*, **52**: 457-468.
- ELLAM R.M. *et alii* (1988) - The transition from calc-alkaline to potassic orogenic magmatism in the Aeolian Islands, Southern Italy. *Bull. Volcanol.*, **30**: 386-398.
- ERICKSON A.J. (1970) - Heat flow measurements in the Mediterranean, Black and Red Seas. Ph. D. Thesis, M.I.T., Cambridge.
- FINETTI M. & DEL BEN A. (1986) - Geophysical study of the Tyrrhenian opening. *Boll. Geofis. Teor e Appl.*, V.28, pp. 75-156.
- FORSYTH D. & UYEDA S. (1975) - On the relative importance of the driving forces of plate motions. *Geophys. J. R. Astr. Soc.*, **43**: pp.163-200.
- FRANCALANCI L., TAYLOR S.R., MCCULLOCH M.T. & WOODHEAD J. (1993) - Petrological and geochemical variations in the calc-alkaline rocks of Aeolian arc (Southern Tyrrhenian Sea, Italy). *Contrib. Mineral. Petrol.*, **113**: 300-313
- GASPARINI C., IANNACONE G., SCANDONE P. & SCARPA R. (1982) - Seismotectonics of the Calabrian Arc. *Tectonophysics*, **84**: 267-286.
- GIARDINI D. & VELONÀ M. (1991) - The deep seismicity of the Tyrrhenian Sea. *Terra Nova*, **3**: 57-64.
- GUEGUEN E., DOGLIONI C. & FERNANDEZ M. (1997) - Lithospheric boudinage in the Western Mediterranean back-arc basins. *Terra Nova*, **9**, 4, 184-187.
- HUTCHINSON I., VON HERZEN R.P., LOUDEN K.E., SCLATER J.G. & JEMSEK J. (1985) - Heat flow in the Balearic and Tyrrhenian basins, Western Mediterranean. *Journal of Geophysical Research*, v.90, pp.685-702.
- KASTENS K., MASCLE J., AUROUX C., BONATTI E., BROGLIA C., CHANNELL J., CURZI P., EMEIS K.C., GLACON G., ASEGAWA S., HIEKE W., MASCLE G., MCCOY F., MCKENZIE J., MENDELSON J., MULLER C., RÉHAULT J.P., ROBERTSON A., SARTORI R., SPROVIERI R. & TORII M., (1988) - ODP Leg 107 in the Tyrrhenian Sea: Insights into passive margin and back-arc basin evolution. *Geological Society of American Bulletin*, v.100, pp.1140-1156.
- LOCARDI E. & NICOLICH R. (1988) - Geodinamica del tirreno e dell'Appennino Centro-Meridionale: la nuova carta della Moba. *Memorie Società Geologica Italiana*, **41**: 121-140
- LODDO M. & MONGELLI F. (1974) - Heat Flow in southern Italy and surrounding seas. *Boll. Geof. Teor. Appl.*, 115-122.
- MALINVERNO A. & RYAN W.B.F. (1986) - Extension in Tyrrhenian Sea and shortening in the Apennines as a result of arc migration driven by sinking of the lithosphere. *Tectonics*, **5**: 2, pp. 227-245.
- MALINVERNO A., CAFIERO M., RYAN W.B.F. & CITA M.B. (1981) - Distribution of Messinian sediments and erosional surfaces beneath the Tyrrhenian Sea: geodynamical implications. *Oceanol. Acta*, **4**: 489-496.
- MALINVERNO A. (1981) - Quantitative estimates of age and Messinian paleobathymetry of the Tyrrhenian Sea after seismic reflection, heat flow and geophysical models. *Boll. Geof. Teor. Appl.*, **23**: 159-171.
- MANTOVANI E. (1982) - Some remarks on the driving forces in the evolution of the Tyrrhenian basin and Calabrian Arc. *Earth Evol. Sci.* 3,266-170.
- MCKENZIE D. P. (1978) - Some remarks on the development of sedimentary basins. *Earth Planet. Sci. Lett.*, **40**: 25-32.
- MONGELLI F. (1991) - Rethickening of the lithosphere after simple stretching in the Tuscan-Latinal pre-apenninic belt. *Boll. Geof. Teor. Appl.*, XXXIII, **129**: 61-67.
- MONGELLI F. & ZITO G. (1994) - Thermal aspects of some geodynamical models of Tyrrhenian opening. *Boll. Geof. Teor. e Appl.*, Vol. XXXVI, 141-144, pp. 21-28.
- MORELLI C., PISANI M. & GANTAR C. (1975) - Geophysical anomalies and tectonics in the Strait of Sicily and of the Ionian Sea. *Boll. Geof. Teor. e Appl.*, v. XVII, **67**: pp. 211-249.
- MORELLI C. (1970) - Physiography, Gravity and magnetism of the Tyrrhenian Sea. *Boll. Geof. Teor. e Appl.*, v. XII, n. **48**: pp. 275-311.
- MORELLI C. (1981) - Gravity anomalies and crustal structures connected with the Mediterranean margins. In: WEZEL F.C. (Ed): "Sedimentary Basins of Mediterranean Margins". C.N.R. Italian Project of Oceanography, Tecnoprint, Bologna, 33-53.
- MORELLI C. (1995) - Ulteriori vincoli geofisici, petrografici e geodetici alla geodinamica del Mediterraneo centrale. *Atti XIII Conv. Naz. del GNGTS*, Vol.1, 27-43.
- PARSONS B. & SCLATER J.G. (1977) - An analysis of the variation of ocean floor bathymetry and heat flow with age. *J. Geoph. Res.*, **82**: 803-827.
- PASCUCCI V., MERLINI S., MARTINI P. (1999) - Seismic stratigraphy of the Miocene-Pleistocene sedimentary basins of the Northern Tyrrhenian Sea and western Tuscany (Italy). *Basin Res.*, **11**: 337-356.
- PATACCA E., SARTORI R. & SCANDONE P. (1990) - Tyrrhenian basin and Apenninic Arcs: Kinematic relations since Late Tortonian times. *Memorie della Società Geologica Italiana*, v.45, pp.453-462.
- PATACCA E. & SCANDONE P. (1989) - Post-Tortonian mountain building in the Apennines. The role of the passive sinking of a relic lithospheric slab. In BORIANI A., BONAFEDE M., PICCARDO G.B. & VAI G.B. (Eds.): "The Lithosphere in Italy". *Accademia Nazionale Lincei*, **80**: 157-176.
- PONTEVIVO A. & PANZA G.F. (2002) - Group velocity tomography and regionalization in Italy and bordering areas. *Phys. Earth Plan. Int.*, **134**: 1-15.
- PFINNER O.A. (1990) - Crustal shortening of the Alps along the EGT profile. In FREEMAN R., GIESE P. & MUELLER ST. (Eds): "The European Geotransverse: Integrative studies". *Eur. Sci. Found.*, Strasbourg, pp. 255-262
- SARTORI R. (1989) - Evoluzione neogenico-recente del bacino tirrenico ed i suoi rapporti con la geologia delle aree circostanti. *Gior. Geol.*, **3**: 51/2, 1-39.
- SCANDONE P. (1980) - Origin of the Tyrrhenian Sea and Calabrian Arc. *Bollettino Società Geologica Italiana*, **98**: 27-34.
- SCLATER J.G. (1972) - Heat flow and elevation of the marginal basins of the western Pacific. *J. Geoph. Res.*, **77**: 5075-5083.
- SELVAGGI G. & CHIARABBA C. (1995) - Seismicity and P-wave velocity image of the Southern Tyrrhenian subduction zone.

- Geophys. J. Int., **121**: 818-826.
- SELVAGGI G. (2001) – *Strain pattern of the Southern Tyrrhenian slab from moment tensors of deep earthquakes: implications on the down-dip velocity*. Ann. Geof., **44** (1): 155-165.
- TURCOTTE D.L. & SCHUBERT G. (1982) - *Geodynamics. Application of continuum Physics to geological problems*. John Wiley, New York.
- YE S. & ANSORGE J. (1990) – *A crustal section through the Alps derived from the EGT seismic refraction data*. In FREEMAN R., GIESE P. & MUELLER ST. (Eds): “*The European Geotransverse: Integrative studies*”. Eur. Sci. Found., Strasbourg, pp. 221-236
- ZITELLINI N., TRINCARDI F., MARANI M., TRAMONTANA M. & BARTOLE R. (1986) - *Neogene tectonics of the Northern Tyrrhenian Sea*. Giorn. Geol., **48**: 25-40.
- ZITO G., MONGELLI F. & LODDO M. (1993) – *Temperature dependence of the thermal parameters of some rocks*. Boll. Geof. Teor. Appl., **140**: 437-445.
- ZOTH G. & HAENEL R. (1988) *Appendix of the Handbook of terrestrial heat-flow density determination*. HAENEL R., RYBACH L. & STEGENA L. (Eds). Kluwer Academic Publishers, Dordrecht (Holland), 499-453.



